

# Potential earthquake locations in India determined by pattern recognition and seismicity modeling

**A. Gorshkov<sup>1</sup>, I.Vorobieva<sup>1</sup>, Mandal<sup>2</sup>, O. Novikova<sup>1</sup>**

*<sup>1</sup>Institute of Earthquake Prediction Theory and Mathematical Geophysics, Russian Academy of Sciences, 84/32 Profsovnaya, Moscow 117997, Russia*

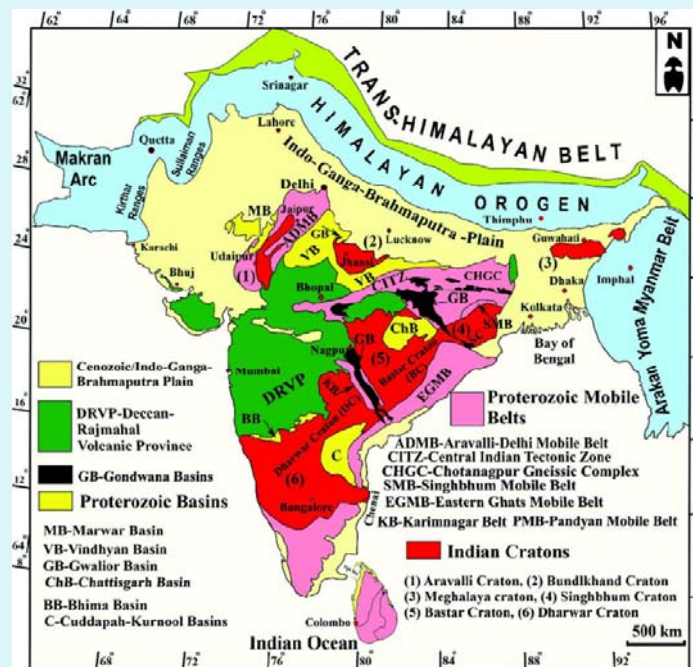
*<sup>2</sup>CSIR-National Geophysical Research Institute, Uppal Road, Hyderabad-500007, A.P., Telengana  
India*

**India - Russia  
Scientific Webinar on  
"Seismology: Monitoring and Forecasting"**

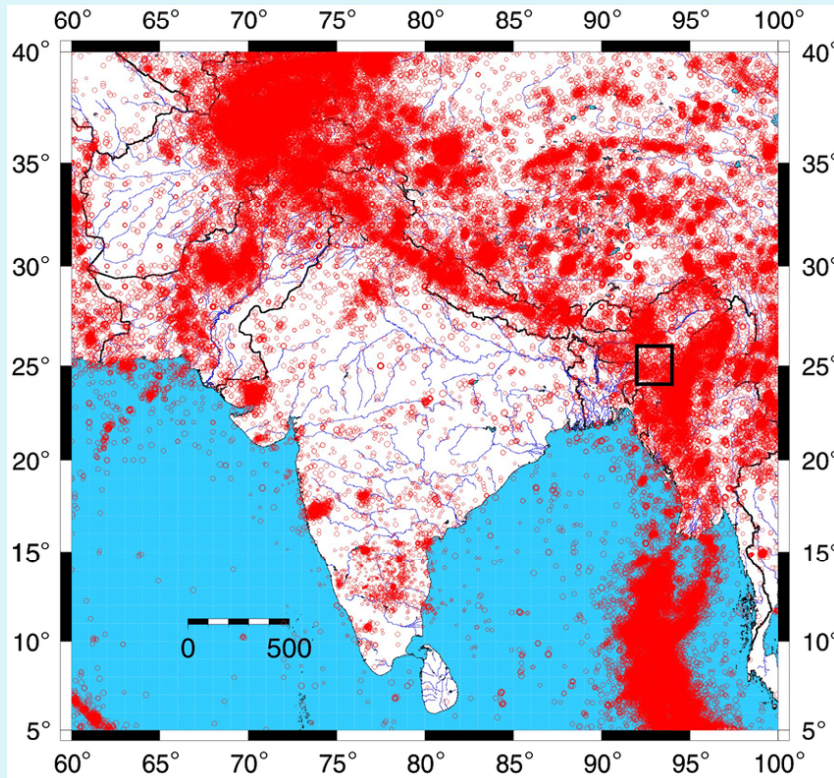
**30 June 2022**

---

# Topography and Tectonic units



# Seismicity and Seismic Zoning



## Seismic Zone Map of India: -2002

About 59 percent of the land area of India is liable to seismic hazard damage

Zone	Intensity
Zone V	<b>Very High Risk Zone</b> Area liable to shaking Intensity IX (and above)
Zone IV	<b>High Risk Zone</b> Intensity VIII
Zone III	<b>Moderate Risk Zone</b> Intensity VII
Zone II	<b>Low Risk Zone</b> VI (and lower)

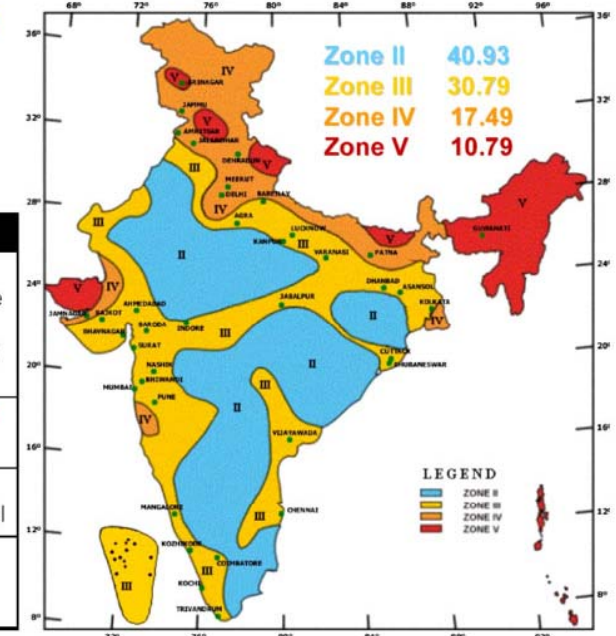
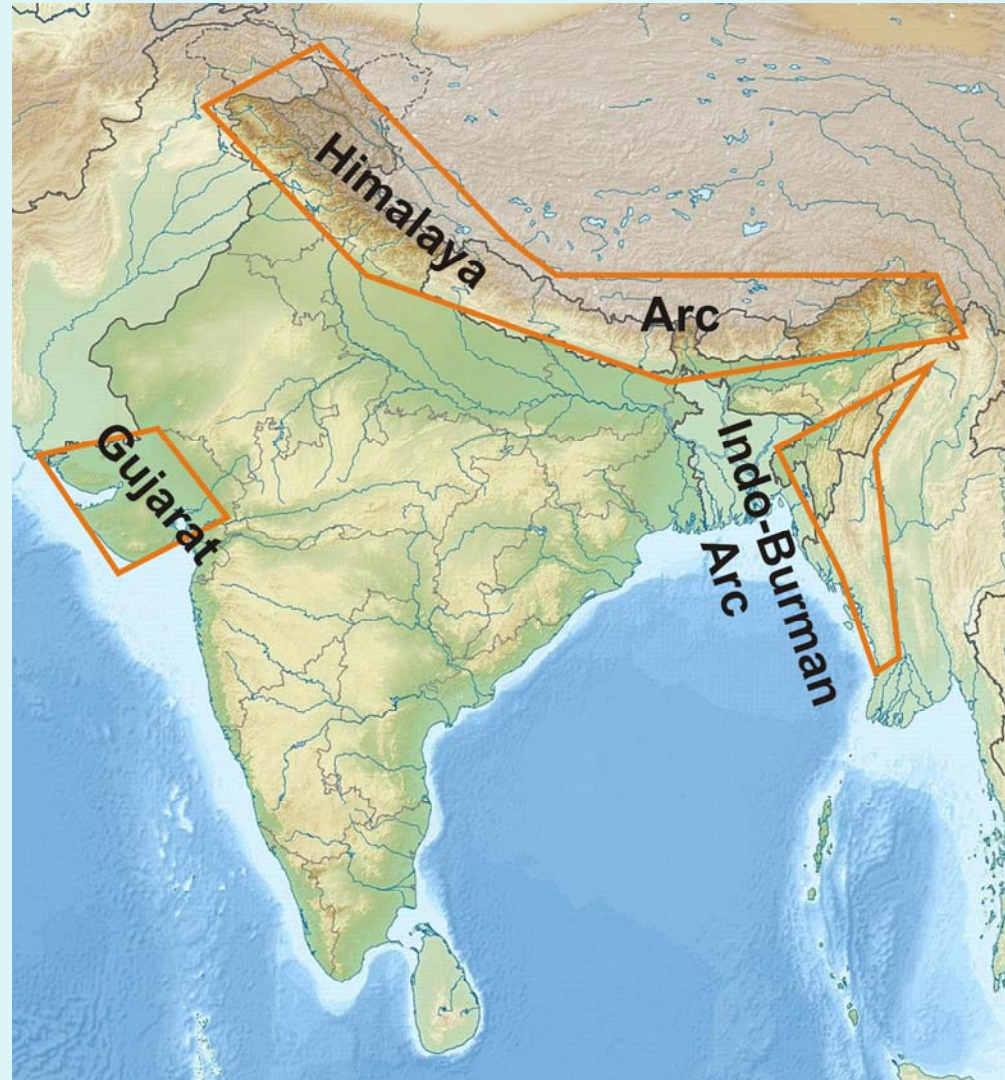


Fig. 1 Seismic zonation and intensity map of India

## Studied regions



## OUTLINE

The results obtained within the framework of the long-term Russian-Indian cooperation in identifying seismically hazardous zones using the methods of **pattern recognition and seismicity modeling** are summarized.

The structural basis for the performed studies was the map of the morphostructural zoning of India (Bhatia et al., 1994; Rantsman et al., 1996).

### Recognition of seismogenic nodes

Seismogenic nodes were identified by pattern recognition technique in the **Himalayan arc** for M6.5+ (Bhatia et al., 1992) and for M7+ as well as in **Gujarat** for M5+ (Gorshkov et al., 2022).

### Seismicity modeling

To better understand the seismic hazard, we applied a **block and fault dynamics (BAFD) model** for the **Himalaya** (Vorobieva et al., 2017) and **Indo-Burman arcs** (Vorobieva et al., 2021) as well as for the **Kachchh rift zone** (Vorobieva et al., 2014) to simulate regional seismicity. The input to the simulation was based on the results of morphostructural analysis to identify crustal blocks, and available GPS observations of tectonic movements in each region.



**Pattern recognition  
applied to seismogenic nodes  
identification**

# Methodology of identifying seismogenic nodes

For identifying seismogenic nodes we employ a phenomenological approach structured according to a **pattern recognition scheme** and based on the **assumption that earthquakes nucleate at nodes**, specific structures forming around intersections of morphostructural lineaments.

## STEP 1:

Delineation of morphostructural nodes with **morphostructural zoning (MZ) method** that outlines hierarchical system of blocks characterized by relative uniformity of the morphostructures

*Compilation of a morphostructural map at the scale of 1: 1,000,000 using the following information:*

- ✓ topographic maps
- ✓ tectonic maps
- ✓ geological maps
- ✓ satellite photos
- ✓ relevant publications

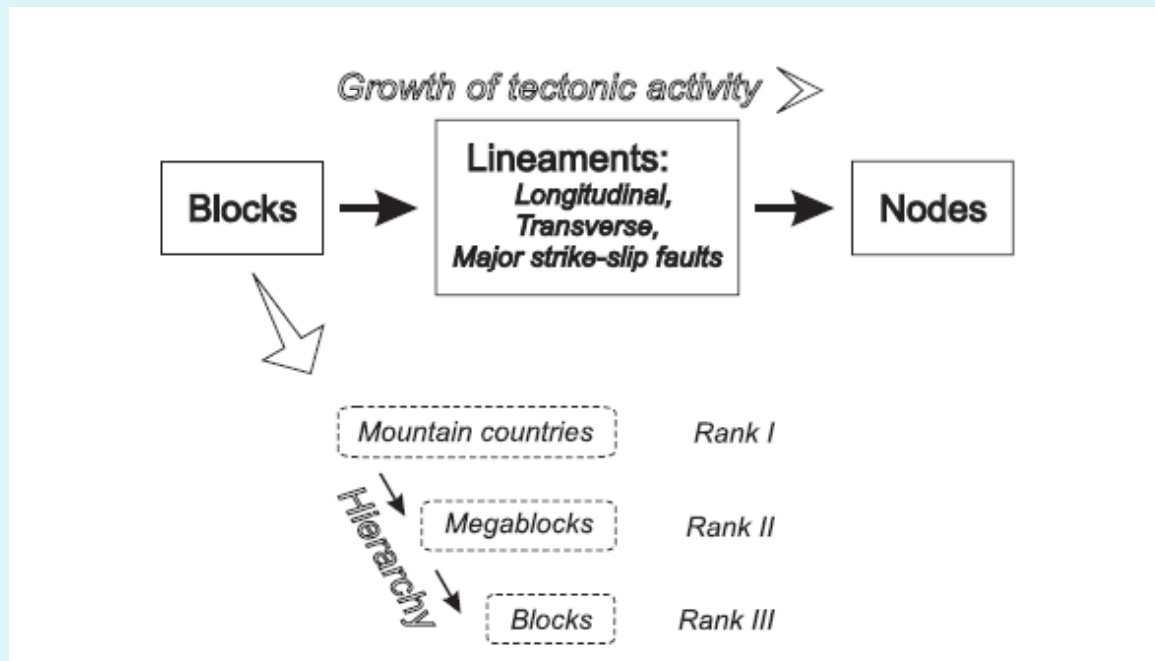
## STEP 2:

Identification of seismogenic nodes on the basis of geomorphic, geological, and gravity data by the **pattern recognition technique**

*Identification of characteristic traits for areas already marked by seismic events ⇒ similarities can be used to identify sites, which did not yet explicitly show up as earthquake-prone.*

# Morphostructural Zoning (MSZ)

The studying objects in recognition of earthquake-prone areas are morphostructural nodes. Their position on the Earth surface is delineated by MSZ based on the analysis of geomorphic, tectonic, geological data with special attention to the present-day topography because the topography is a very sensitive indicator of tectonic deformation both in young orogenic belts and in intraplate areas. In the MSZ, the study region is divided into a system of hierarchically ordered areas, characterized by homogeneous present-day topography and tectonic structure. MSZ distinguishes three interrelated elements of the block-structure (1), areal elements, blocks; (2) linear zones bounding blocks, morphostructural lineaments; and (3) sites of the intersections of the lineaments, the nodes. The nodes are delineated by MSZ that is based on geomorphic and geological data and does not rely on the knowledge about past seismicity. Empirically it was found that strong earthquakes nucleate at nodes.

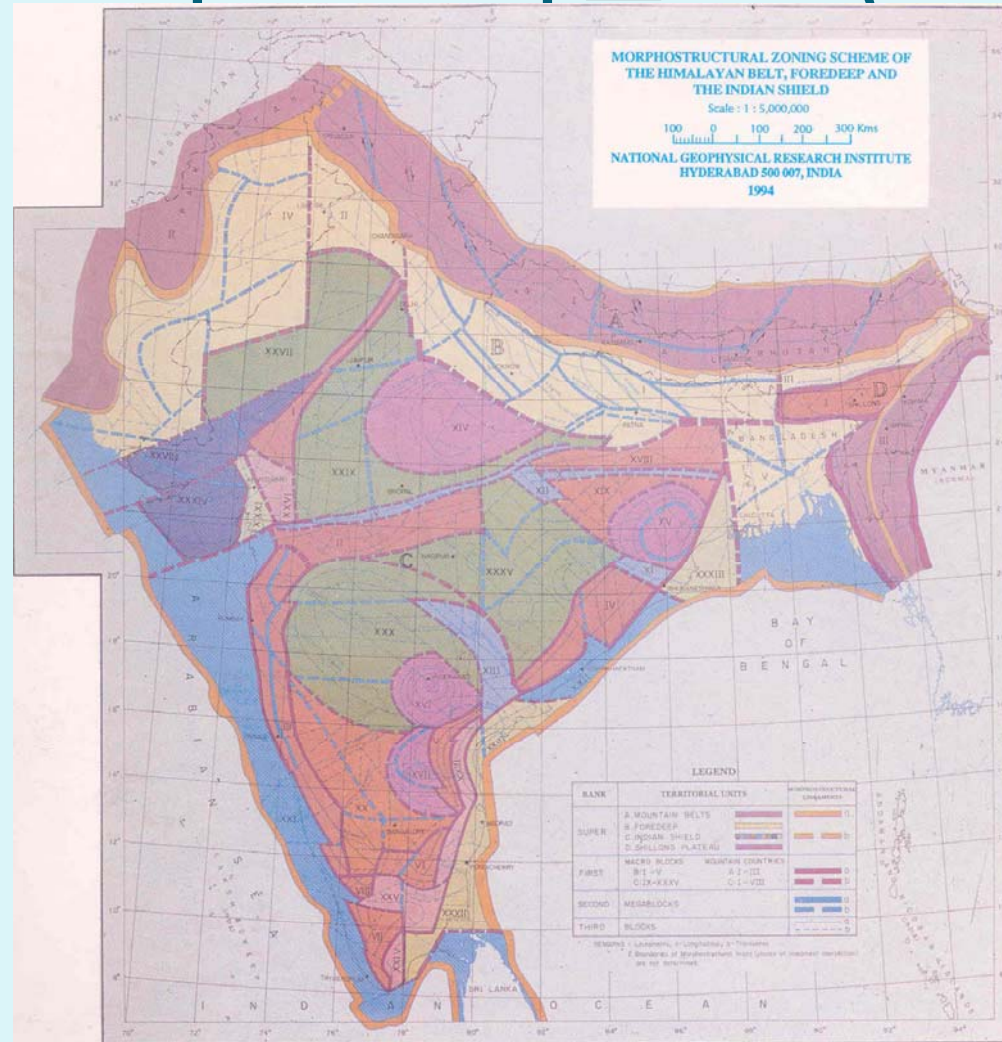


Principal scheme of the morphostructures in MSZ

# Morphostructural map of Indian peninsula (1994)

MZ map was a base for recognizing of seismogenic nodes and block-structure delineating in seismicity modeling.

The map shows hierarchical block-and-lineament geometry of the peninsula.  
Large scale tectonic units are shown by different color.



Chetty, T.R.K., Rao M.N., Gorshkov A.I., Glazko M.P., Rantsman E.Ya., Zhidkov M.P. (1994).  
Morphostructural zoning scheme of the Himalayan belt, foredeep and the Indian shield.  
Scale 1:5,000,000. NGRI, Hyderabad, India

## Parameters of the nodes

(the input for the pattern recognition algorithm CORA 3)

- ***Morphometric parameters***

Maximum height in the node, (Hmax)

Minimum height in the node, (Hmin)

Maximum height difference in the node  
( $\Delta H$ )

Distance between the points Hmax and  
Hmin, (L)

Slope, ( $\Delta H/L$ )

- ***Geological parameters***

The portion of soft (quaternary) sediments

- ***Gravity parameters***

Maximum value of Bouguer anomaly,

Minimum value of Bouguer anomaly,

Difference between Bmax and Bmin

- ***Parameters of lineament-and-block geometry***

Highest rank of lineament in a node

Number of node-forming lineaments

Distance to the nearest 1st rank  
lineament

Distance to the nearest 2nd rank  
lineament

Distance to the nearest node

Parameters indirectly characterize the contrast of neotectonic movements, lineament-and-block geometry, and deep homogeneity of the crust in the vicinities of nodes.

## Learning stage

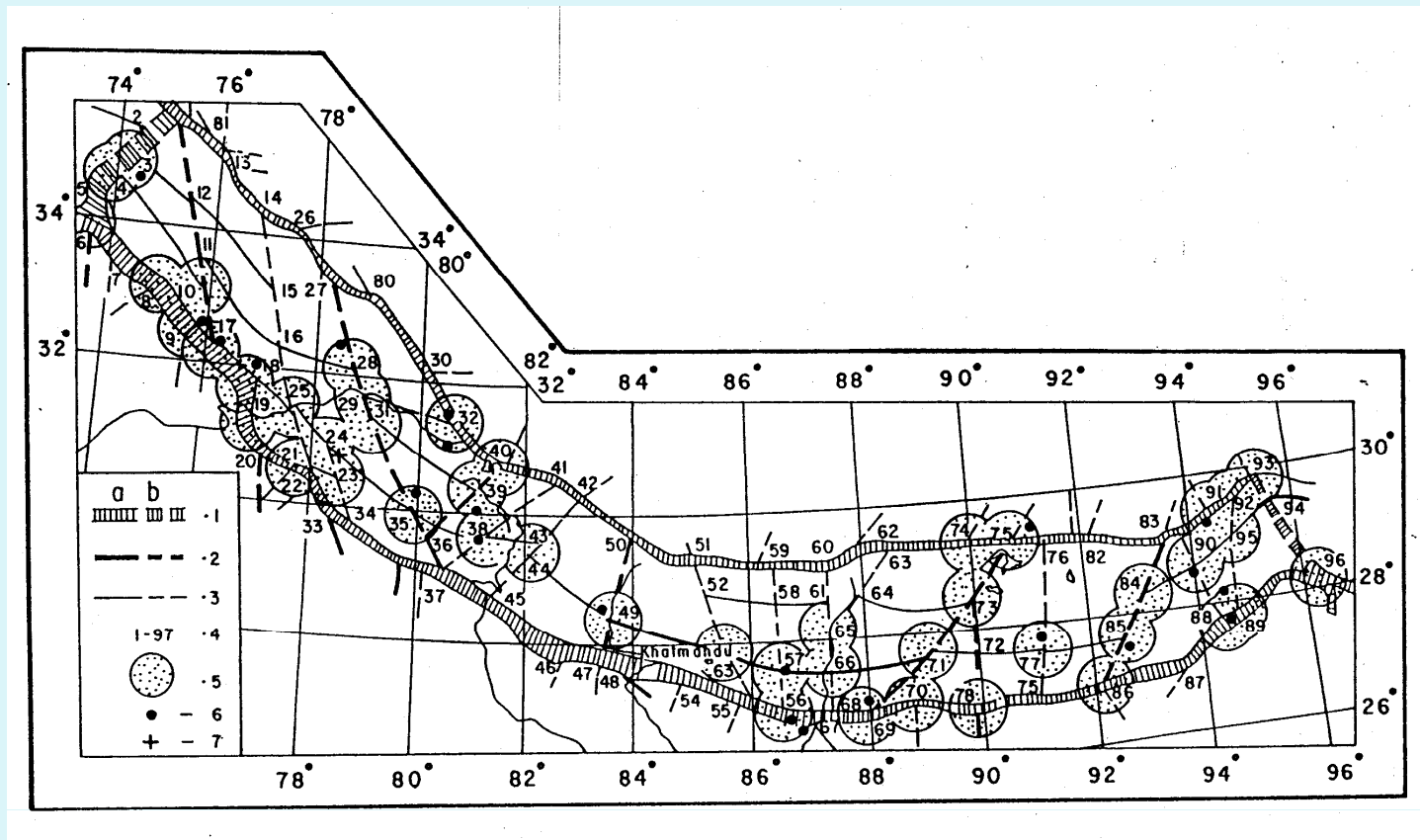
Classification of the entire set of the nodes delineated with MZ into seismogenic (**D**) and non-seismogenic (class **N**) ones for target M is performed by the algorithm CORA-3. This is a recognition algorithm of logical type with learning.

At the learning stage each node is *a priori* assigned to one of the following three sets:

- Set **D**<sub>0</sub> includes nodes hosting instrumental and historical target events
- Set **N**<sub>0</sub> includes nodes, in the vicinities of which there are not recorded target earthquakes of smaller size events
- Set **X** includes nodes, in the vicinities of which there are recorded earthquakes of smaller size

*The set X is not employed for the selection of the characteristic traits; the nodes from the set X are classified at the recognition stage.*

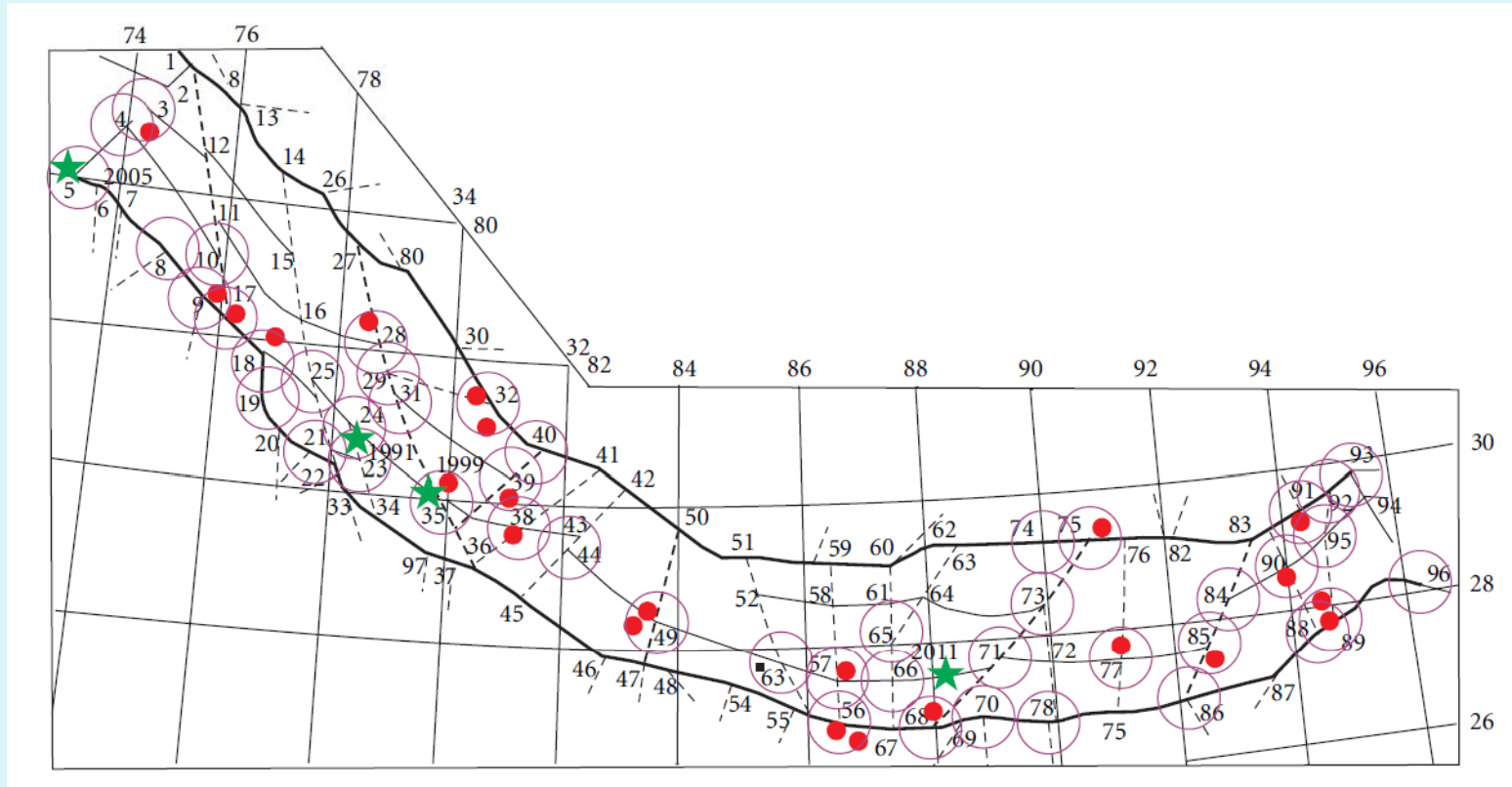
## Seismogenic nodes recognized in Himalaya (M6.5+)



**Circles mark recognized seismogenic nodes**

Bhatia S.C., Chetty T.R.K., Filimonov M., Gorshkov A., Rantsman E., Rao M.N. (1992)  
Identification of Potential Areas for the Occurrence of Strong Earthquakes in Himalayan Arc Region.  
Proc.IndianAcad.Sci.(Earth Planet.Sci). 101 (4), 369-385

## Himalaya: Post-publication events M6.5 (2012)

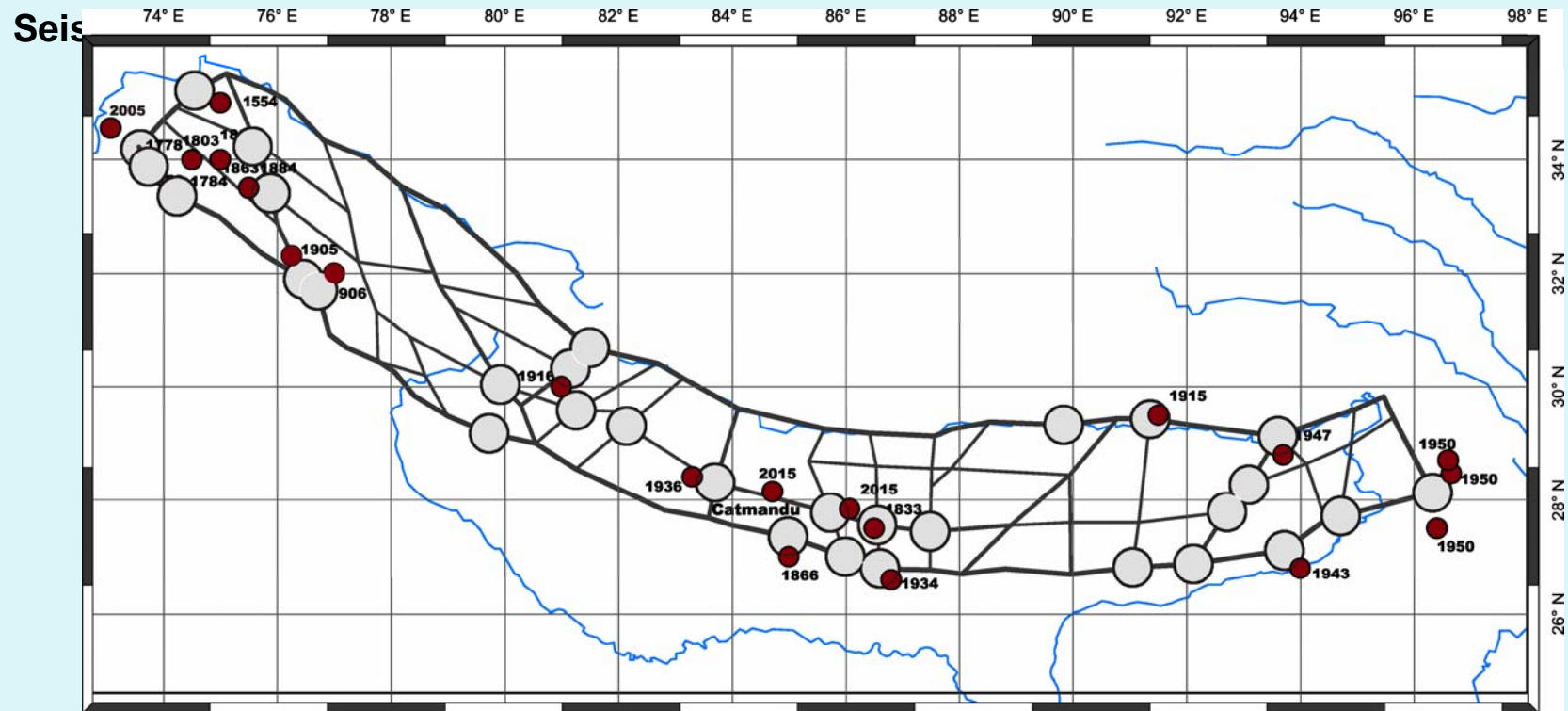


Red dots mark events M6.5+ before 1992

Green stars show events M6.5+ for the period 1992-2012

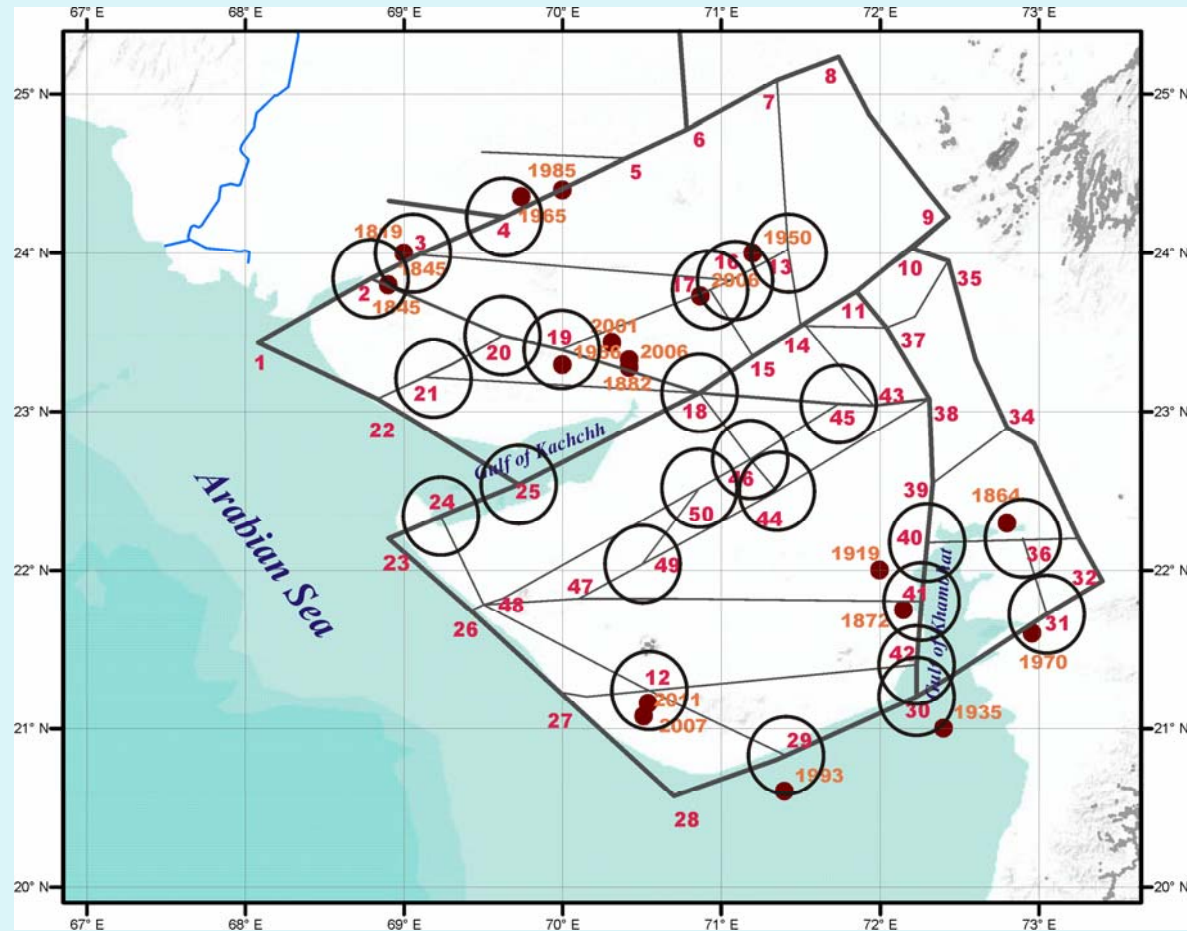
Gorshkov A. Parvez Y., Novikova O. (2012). Recognition of Earthquake-Prone Areas in the Himalaya: Validity of the Results, *International Journal of Geophysics*, vol. 2012, Article ID 419143, 5 pages. doi:10.1155/2012/419143

# Seismogenic nodes for M7+ in Himalaya



Red dots mark epicenters M7+  
Grey circles depict capable nodes for M7+

## Seismogenic nodes recognized in Gujarat (M5+)



**Circles mark recognized seismogenic nodes**

Gorshkov A., Hassan H.M., Mandal P. Novikova O. (2022) Identifying Potential Earthquake Sources in Continental Environments. *SurvGeophys*, <https://doi.org/10.1007/s10712-021-09683-z>



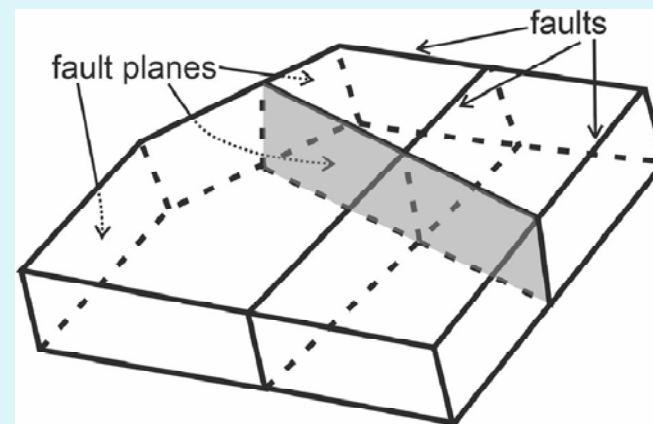
# Seismicity modeling

## The Block-and-Fault Dynamics Model (BAFD)

The Block-and-Fault Dynamics Model (BAFD) that was developed to simulate regional lithosphere dynamics and seismicity. The model is designed under the hypothesis that the structure of a region, fault kinematics, and the statistics of regional seismicity are fundamentally interrelated. The region is modeled as a system of rigid crustal blocks separated by thin visco-elastic faults, which move in response to external tectonic and basal motions. The advantage of BAFD dynamic model is that it simulates both slow tectonic motions and earthquake sequences. It allows studying a wide range of problems from testing of geodynamic hypotheses to seismic risk assessment.

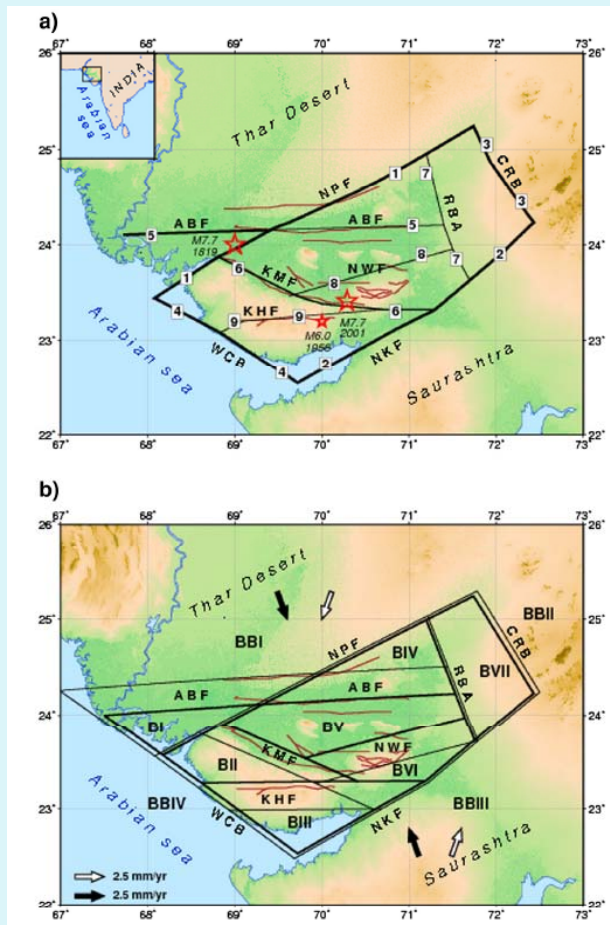
The method allows us to use a realistic geometry of the blocks, based on any relevant information, in particularly maps of morphostructural zoning. In BAFD modeling, driving tectonic forces (velocities of the boundary blocks and underlying medium) are prescribed using geodetic data (GPS) and geodynamic models. The rheology of fault zones can also be incorporated using the existing knowledge of lithospheric structure (in terms of crust–mantle structure and velocities of seismic wave propagation) and heat flow data.

### A block-and-fault structure in BAFD models



The model is described in details by Soloviev A, Ismail-Zadeh A (2003) Models of dynamics of block-and-fault systems. In: Keilis-Borok VI, Soloviev AA (eds) Nonlinear dynamics of the lithosphere and earthquake prediction. Springer, pp 71-138

# Block structure of the Kachchh rift zone



Block structure of the Kachchh rift zone.

a) Morphostructural zoning map. Black lines depict lineaments. 1–1 to 9–9 — numbers of lineaments. Red lines mark geologically mapped faults (Biswas, 1987; Mandal et al., 2004): the Cambay Rift Basin (CRB), Kachchh Mainland Fault (KMF), South Wagad Fault (SWF), North Kathiawar Fault (NKF), West Coastal boundary (WCB), Kachchh Hill Fault (KHF), Allah Bund Fault (ABF), North Wagad Fault (NWF), Radhanpur–Barmer Arch (RBA), and Nagar Parkar Fault (NPF).

b) Geometry of the block structure for modeling. Thick and thin lines depict the model faults on the surface and on the bottom of the structure, respectively. Names of the model faults correspond to the names of the geological faults and structural boundaries. BI–BVII — blocks, BB1–BBIV — boundary blocks. Open and filled arrows show direction of in-plane compression for two variants of modeling

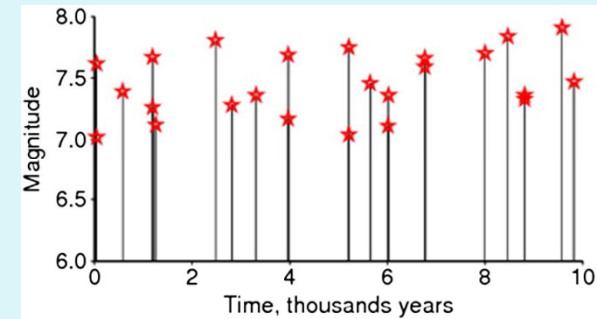
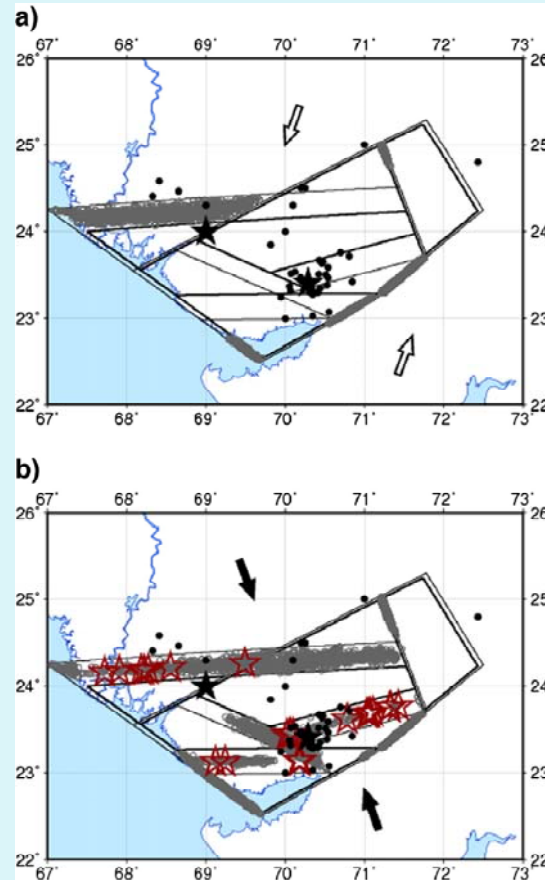
# Parameters for modeling

Geometrical parameters for BAFD modeling of the Kachchh rift zone.

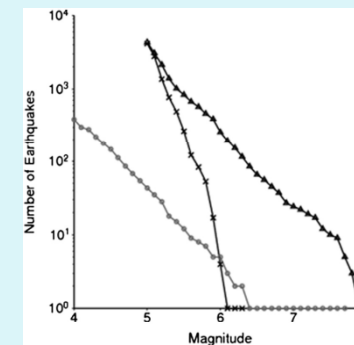
Parameter	Element of BAFD	Specified value	Values from observations and studies	Reference	
Geometry of block structure	Entire structure	Fig. 1	MZ map	Bhatia et al. (1994)	
Dip angles of faults	NPF, RBA, NKF (east and west)	85°	Sub-vertical	Biswas (1987, 2005)	
		80°	Sub-vertical	Biswas (1987), Biswas (2005)	
	KMF	60°, south	55°–70°, south	Mandal and Horton (2007)	
	KHF	50°, south	41°–55°, south	Chung and Gao (1995),	
	NWF	50°, south	40°–61°, south	Mandal et al. (2009)	
Thickness of the block structure	Entire structure	ABF	50°, north	45°–55°, north	Mandal et al. (2009)
		38 km	Moho depth	36–42 km	Mandal (2012)

# Modeling results for Kachchh rift zone

The modeling shows that epicenter distribution, nucleation of large earthquakes and the slope of the FMD are sensitive to the changes in the orientation of driving forces in the Kachchh rift zone. The main result from the block modeling suggests that an **NNW–SSE trending compression** is a principal driving force that explains basic features of the regional seismicity. Specifically, the nucleation of large synthetic events on the fault segments is associated with the faults which are the causative faults for the 1819 Allah-Bund, 1956 Anjar and 2001 Bhuj earthquakes, respectively

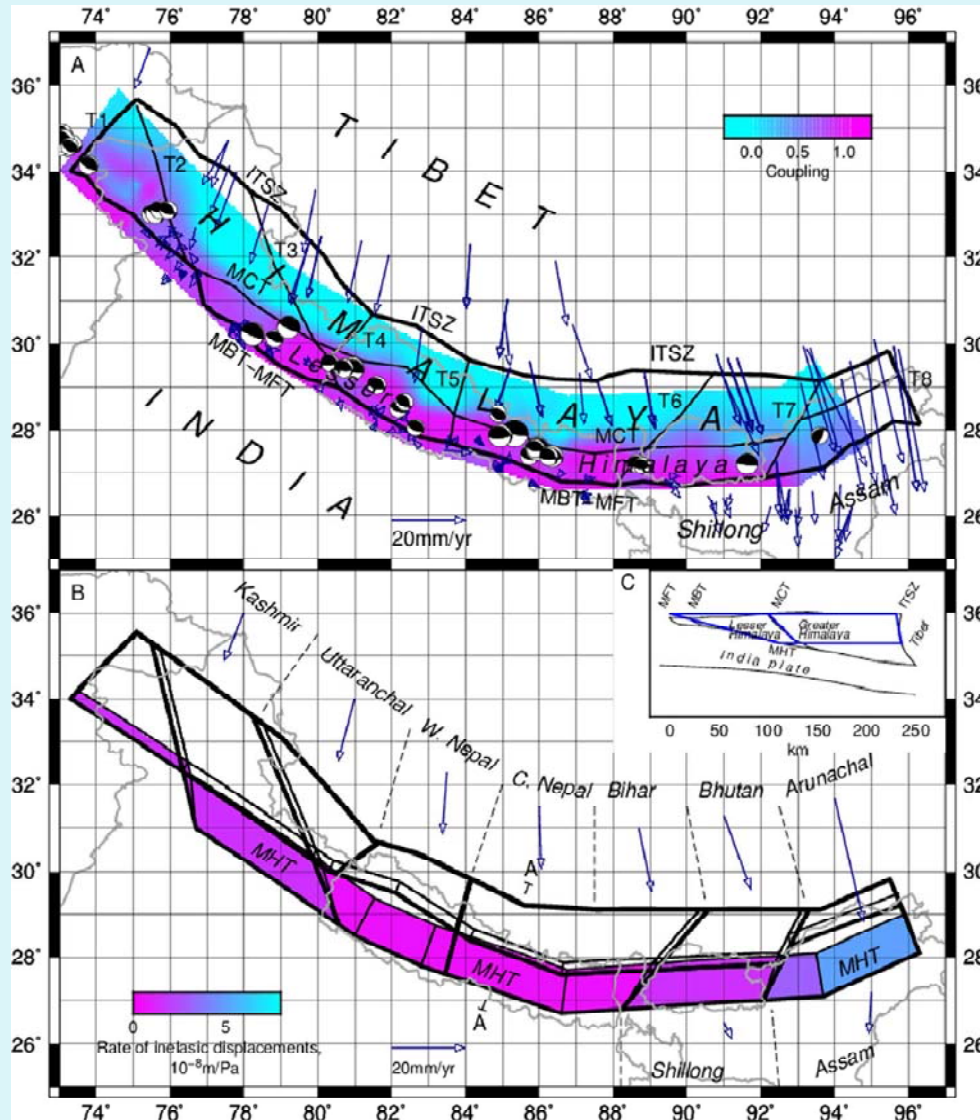


Time sequence of the synthetic earthquakes with  $M \geq 7$  generated in 10 thousand years with **NNW–SSE compression**. Recurrence time varies from less than 1 year to 1600 years. Average rate is 2.5 events per 1000 years.



The FMDs for both synthetic (right curve) and observed seismicity (left curve) have a similar slope of magnitude–frequency relation or b-value.

# Seismicity modeling in Himalaya (block-structure)

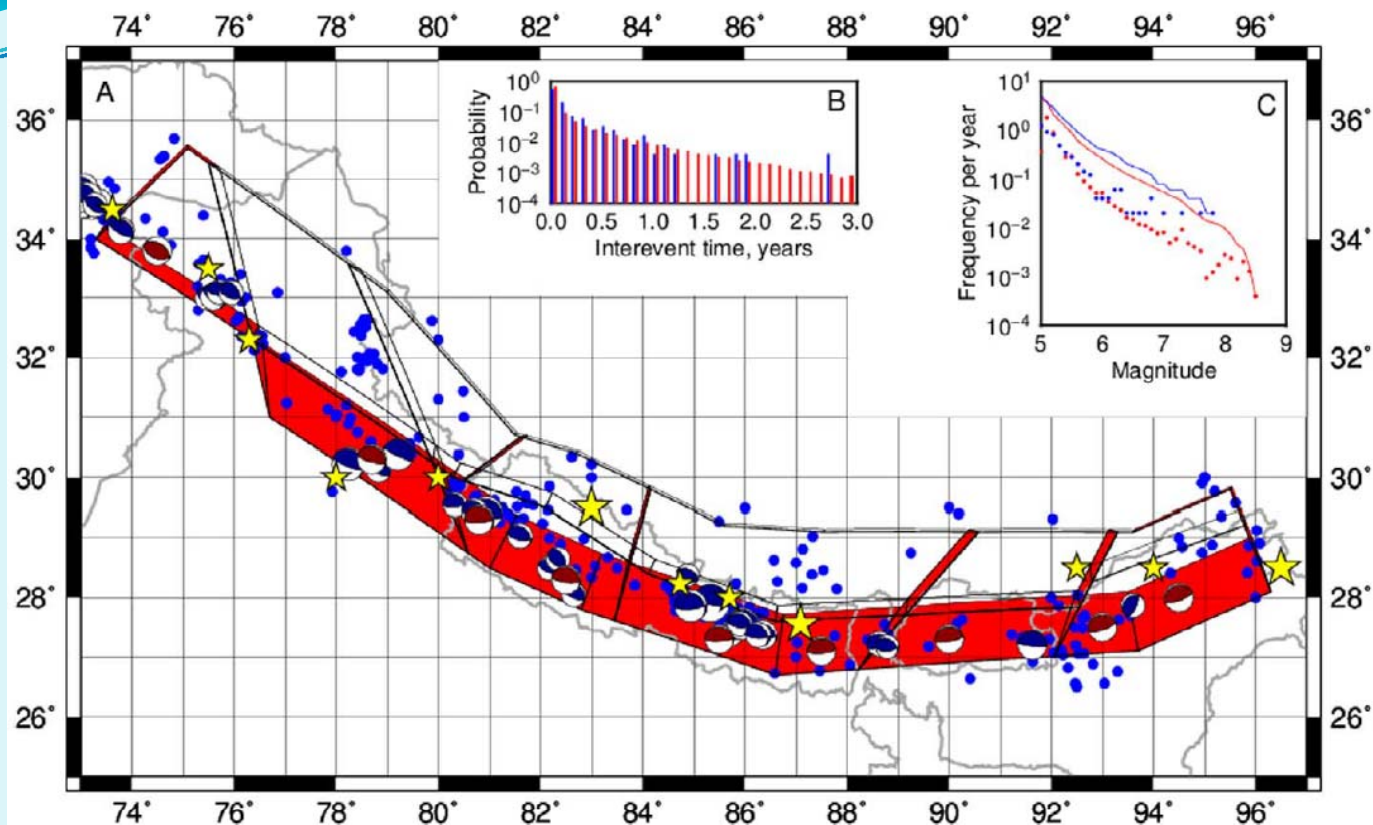


Geophysical observation and studies in the Himalaya and input parameters for BADF modeling.

A) Black lines show lineaments of the Himalaya defined by MZ map, blue arrows – tectonic velocities in the stable India frame (Vernant et al., 2014), beach-balls – selected FPSs of Himalayan earthquakes (CMT global catalogue).

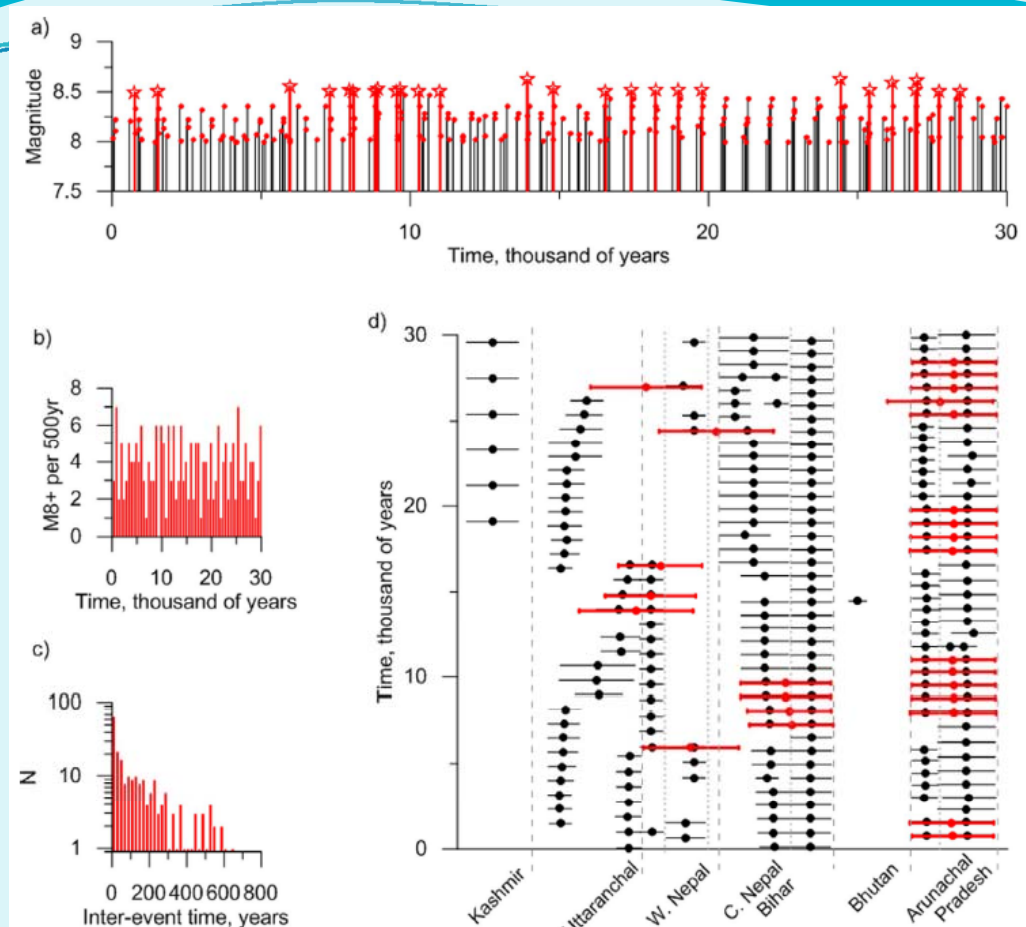
B) Black lines – geometry of the block structure (thick-surface, thin-bottom), colour map – rate of inelastic displacements in MHT, blue arrows – external velocities.

C) Schematic cross-section of Himalaya (simplified after Elliott et al., 2016).



A plot showing fundamental characteristics of the synthetic seismicity and its comparison with observations.

- A) Seismically active segments of the block structure are shown in red. Blue dots mark recorded earthquakes with  $M \geq 5.0$ , 1500–2015, yellow stars – significant Earthquakes  $M7.5+$ . Blue beach balls depict the selected FPS of the Himalayan earthquakes (CMT global catalogue); red beach balls show typical FPSs of the synthetic earthquakes in the corresponding segments of MHT.
- B) Distribution of interevent times for synthetic (red), and recorded (blue) earthquakes  $M \geq 5.0$ , 1966–2015.
- C) Frequency-magnitude distributions per year for synthetic (red) and recorded (blue) earthquakes of  $M \geq 5.0$ , during 1966–2015, cumulative and non-cumulative plots are shown by line and dots, respectively.



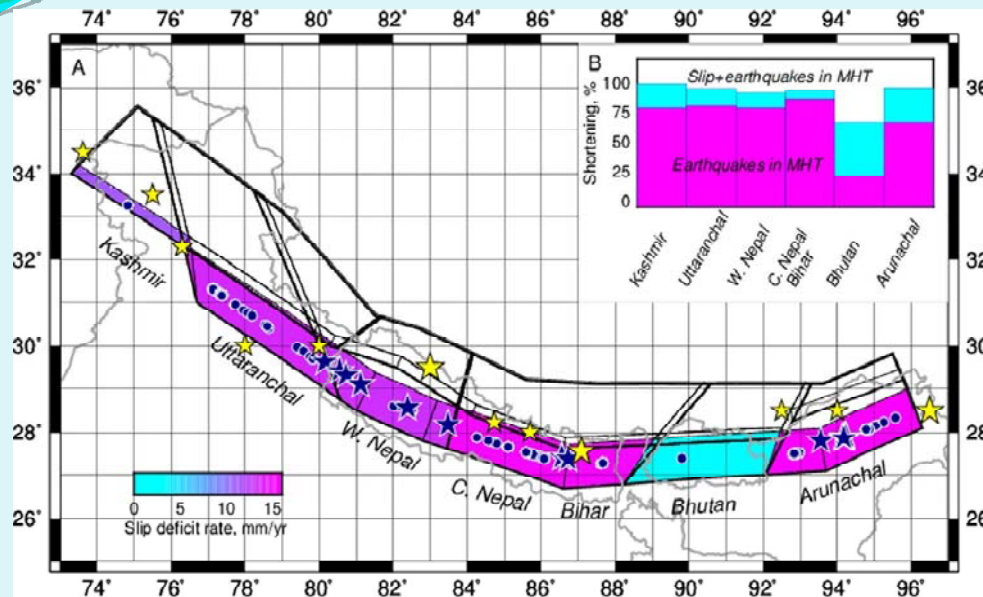
A plot showing temporal statistics of great synthetic earthquakes of M8+.

a) – time sequence;

b) some M8+ synthetic earthquakes per 500 years; c) distribution of inter-event times;

d) time-space sequences of M8+ earthquake sources in MHT. Multisegment earthquakes of M8.5+ are highlighted by red in a) and d).

## Modeling results for Himalaya (Vorobieva et al., 2017)



Great synthetic and observed earthquakes in Himalaya.

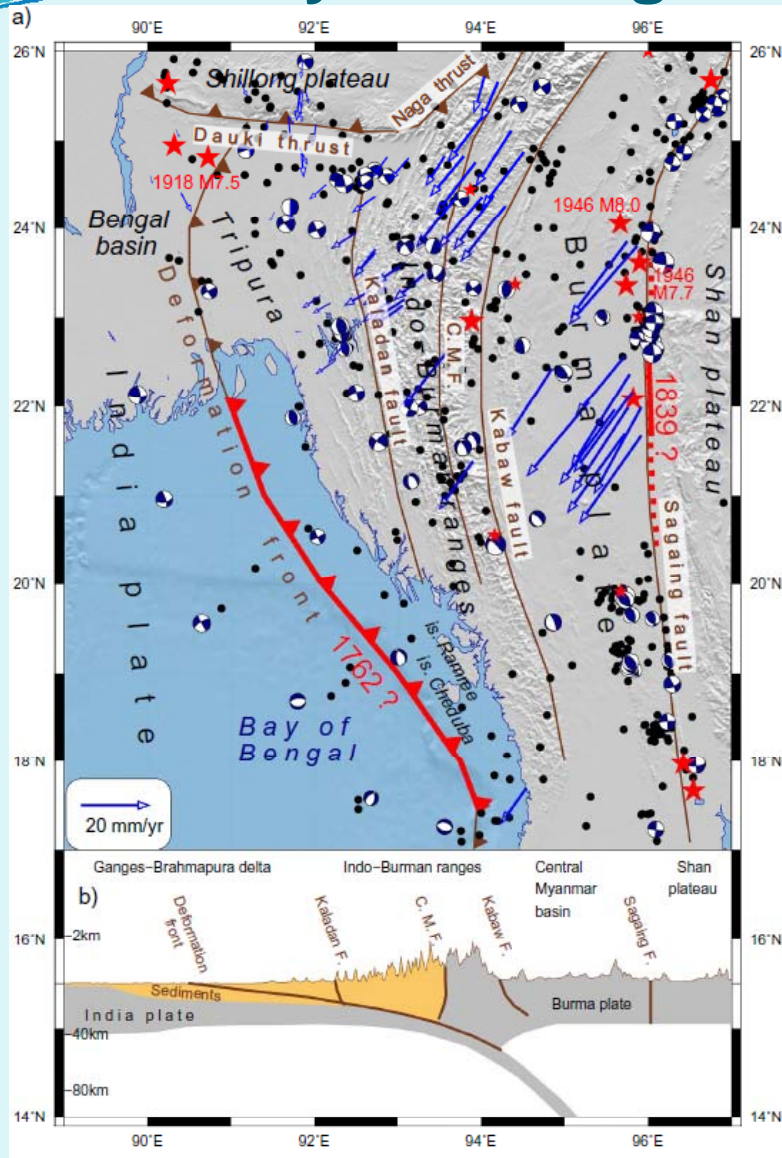
A) Blue circles – synthetic earthquakes M8+, blue stars- multi-segment events M8.5+. Yellow stars show observed significant earthquakes of M7.5+ occurred during 1500–2015. Larger stars show events of M8+. The colour map marks the slip deficit rate.

B) The portion of total shortening across Himalaya arc, which accommodates in the MHT (cyan bar chart), and the portion of slip released by earthquakes in MHT in six sections of Himalaya (magenta bar chart).

In spite of significant simplification, the BAFD modeling reproduces integral features of instrumentally recorded seismicity and basic geodynamics of the Himalayan frontal arc, which includes the accommodation of the large portion of the shortening across the Himalaya within the MHT (Elliott et al., 2016) and predominant seismic release of the accumulated slip deficit (Avouac et al., 2001). The location of great synthetic earthquakes and their maximum magnitudes are consistent with instrumental and historical records. We also reproduce a time clustering of the significant earthquakes, which was found in the XIII-XVI centuries, and is observed nowadays. We modeled seismic cycles in all the sections of the Himalaya and obtained return periods, which show good correlations with return period estimates from recorded earthquakes and paleoseismological studies.

Based on the BAFD modelling, we suppose that the presently observed series of great earthquakes in the Himalaya can continue in any place between the 1905 Kangra and the 2015 Gorkha ruptures, while significant large/great events are less probable in the Kashmir and Assam gaps.

# Seismicity modeling in the Indo-Burman arc



## Comprehensive overview of the Indo-Burman megathrust.

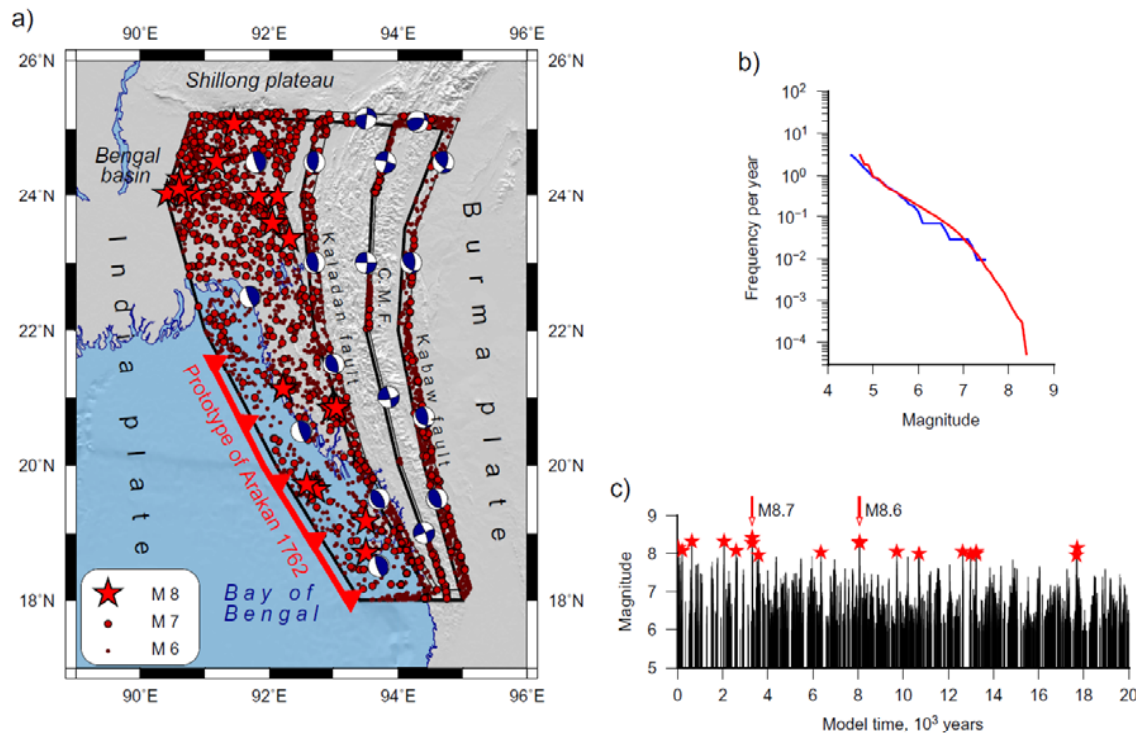
(a) Major faults are shown in brown, CMF is Churachandpur-Mao fault; Black dots and red stars mark shallow ( $h < 40$  km) earthquakes with  $M \geq 4.5$  (1973–2020) and  $M \geq 6.5$  (1900–2007) (ANSS, Centennial catalog).

Beach-balls are Fault Plane Solutions (FPS) (GCMT); blue arrows show GPS velocities relative to stable India. Possible ruptures of the 1762 Arakan earthquake and the 1839 Ava earthquake are traced by red. (b) Schematic cross-section at latitude  $24^\circ$  N,

## Parameters of the model

Dip angles of faults are prescribed based on the cross-sections. The CMF is a sub-vertical fault with a dip angle of  $80^\circ$ . The Kabaw and Kaladan faults having the complex structure reveal both strike-slip and thrust features. We model them as steeply inclined faults with a dip angle of  $60^\circ$ . The dip angle of the IBD changes from  $10^\circ$  in the north to  $15^\circ$  in the south. The depth of blocks is assumed to be 30 km which corresponds to the locked depth of the IBD in models

# Seismicity modeling in the Indo-Burman arc



Overview of synthetic seismicity simulated for 20 thousand years by the preferred model “All faults locked”.

(a) The map of epicenters: all great earthquakes with  $M \geq 8$  (red stars) are simulated in the India-Burma Detachment (IBD); beach balls are synthetic FPS.

(b) Earthquake size distribution (frequency per year) for the synthetic (red) and recorded (blue) seismicity.

(c) Time sequence of synthetic M6+ earthquakes. The rupture zone of two multi-segment giant M8.7 and M8.6 earthquakes is marked by red thrust line in (a), and by arrows in (c).

The integral characteristics of synthetic seismicity, the earthquake size distribution and the rate of seismic activity are compatible with those derived from the observed seismicity, historical records and paleoseismic studies. Our results suggest that the megathrust is locked and can generate great M8+ earthquakes with a long recurrence period exceeding 1000 years. We modelled two mega-earthquakes with magnitudes 8.7 and 8.6 in the southern section of the Indo-Burman arc, which may be similar to the 1762 Arakan earthquake. This is supported by paleoseismic studies. Additionally, we obtained several M8+ events in the northern onshore section of the megathrust where no great earthquakes have been reported by the instrumental and historical records.

Vorobieva I et al (2021) Modelling the seismic potential of the Indo-Burman megathrust. *Sci Rep* 11, 21200 (2021).

# Conclusions

The results of recognizing seismogenic nodes suggest their sufficient reliability for use in applications related to seismic hazard assessment.

BAFD models of the studied regions reproduces the main features of the observed seismicity, provides potential locations of large earthquakes, and return periods of large size events.

The results obtained make a significant contribution to the seismic hazard assessment and the forecasting of the locations of future earthquakes in the seismic regions of India.

# References

- Bhatia S.C., Chetty T.R.K., Filimonov M., Gorshkov A., Rantsman E., Rao M.N. (1992) Identification of Potential Areas for the Occurrence of Strong Earthquakes in Himalayan Arc Region. Proc.IndianAcad.Sci.(Earth Planet.Sci). 101 (4), 369-385
- Chetty, T.R.K., Rao M.N., Gorshkov A.I., Glazko M.P., Rantsman E.Ya., Zhidkov M.P. (1994). Morphostructural zoning scheme of the Himalayan belt, foredeep and the Indian shield. Scale 1:5,000,000. NGRI, Hyderabad, India
- Gorshkov A. Parvez Y., Novikova O. (2012). Recognition of Earthquake-Prone Areas in the Himalaya: Validity of the Results, International Journal of Geophysics, vol. 2012, Article ID 419143, 5 pages. doi:10.1155/2012/419143.
- Gorshkov A., Hassan H.M., Mandal P. Novikova O. (2022) Identifying Potential Earthquake Sources in Continental Environments. SurvGeophys, <https://doi.org/10.1007/s10712-021-09683-z>
- Rantsman E.Y., Glasko M.P., Gorshkov A.I. (1996) Hierarchy of the present-day block structure of the Indian shield and its orogenic framework. Transactions (Doklady) of the Russian Academy of Sciences. Earth Science Sections. 349 (5), 839-843
- Vorobieva I., Mandal P., Gorshkov A. (2014) Numerical modeling of seismicity and geodynamics of the Kachchh rift zone, Gujarat, India. Tectonophysics, 634 (5) 31-43 <http://dx.doi.org/10.1016/j.tecto.2014.07.0>
- Vorobieva I., Mandal P., Gorshkov A.(2017) Block-and-fault dynamics modeling of the Himalayan frontal arc: Implications for seismic cycle, slip deficit, and great earthquakes, Journal of Asian Earth Sciences, 148, 131-141 doi: <http://dx.doi.org/10.1016/j.jseaes.2017.08.033>
- Vorobieva I., Gorshkov A. & Mandal, P. (2021) Modelling the seismic potential of the Indo-Burman megathrust. Sci Rep 11, 21200 (2021). <https://doi.org/10.1038/s41598-021-00586-y>